Large-area organic distributed feedback laser fabricated by nanoreplica molding and horizontal dipping

Chun Ge,[1] Meng Lu,[2] Xun Jian,[1] Yafang Tan,[1] and Brian T. Cunningham[1,3,*]

[1]*Dept. of Electrical Engineering, University of Illinois at Urbana-Champaign, Urbana, IL, USA*
[2]*SRU Biosystems, 14-A Gill St., Woburn, Massachusetts, 01810, USA*
[3]*Dept. of Bioengineering, University of Illinois at Urbana-Champaign, Urbana, IL, USA*
**bcunning@illinois.edu*

Abstract: The fabrication of visible wavelength vertically emitting distributed feedback (DFB) lasers with a subwavelength grating fabricated by a replica molding process and an active polymer layer printed by a horizontal dipping process is reported. The combined techniques enable the organic DFB laser to be uniformly fabricated over large surface areas upon a flexible plastic substrate, with an approach that is compatible with roll-based manufacturing. Using a fixed grating period and depth, DFB laser output wavelength is controlled over a 35 nm range through manipulation of the waveguide layer thickness, which is controlled by the speed of the horizontal dipping process. We also demonstrate that the active area of the structure may be photolithographically patterned to create dense arrays of discrete DFB lasers.

OCIS codes: (140.3490) Lasers, distributed-feedback; (250.7270) Vertical emitting lasers; (250.2080) Polymer active devices; (220.4241) Nanostructure fabrication; (310.6860) Thin film, optical properties.

References and links

1. I. D. W. Samuel, and G. A. Turnbull, "Organic semiconductor lasers," Chem. Rev. **107**(4), 1272–1295 (2007).
2. G. Morthier, W. D'Oosterlinck, and K. Huybrechts, "All-optical flip-flops based on DFB laser diodes and DFB-arrays," J. Mater. Sci. Mater. Electron. **20**(S1), 385–389 (2009).
3. C. Ge, M. Lu, W. Zhang, and B. T. Cunningham, "Distributed feedback laser biosensor incorporating a titanium dioxide nanorod surface," Appl. Phys. Lett. **96**(16), 163702 (2010).
4. M. Lu, S. S. Choi, U. Irfan, and B. T. Cunningham, "Plastic distributed feedback laser biosensor," Appl. Phys. Lett. **93**(11), 111113 (2008).
5. H. Rabbani-Haghighi, S. Forget, S. Chenais, A. Siove, M.-C. Castex, and E. Ishow, "Laser operation in nondoped thin films made of a small-molecule organic red-emitter," Appl. Phys. Lett. **95**(3), 033305 (2009).
6. N. Tsutsumi, A. Fujihara, and D. Hayashi, "Tunable distributed feedback lasing with a threshold in the nanojoule range in an organic guest-host polymeric waveguide," Appl. Opt. **45**(22), 5748–5751 (2006).
7. T. Riedl, T. Rabe, H.-H. Johannes, W. Kowalsky, J. Wang, T. Weimann, P. Hinze, B. Nehls, T. Farrell, and U. Scherf, "Tunable organic thin-film laser pumped by an inorganic violet diode laser," Appl. Phys. Lett. **88**(24), 241116 (2006).
8. D. Schneider, T. Rabe, T. Riedl, T. Dobbertin, M. Kroger, E. Becker, H.-H. Johannes, W. Kowalsky, T. Weimann, J. Wang, and P. Hinze, "Ultrawide tuning range in doped organic solid-state lasers," Appl. Phys. Lett. **85**(11), 1886–1888 (2004).
9. S. Riechel, U. Lemmer, J. Feldmann, S. Berleb, A. G. Mückl, W. Brütting, A. Gombert, and V. Wittwer, "Very compact tunable solid-state laser utilizing a thin-film organic semiconductor," Opt. Lett. **26**(9), 593–595 (2001).
10. L. Xue, S. R. J. Brueck, and R. Kaspi, "Widely tunable distributed-feedback lasers with chirped gratings," Appl. Phys. Lett. **94**(16), 161102 (2009).
11. B. J. Scott, G. Wirnsberger, M. D. McGehee, B. F. Chmelka, and G. D. Stucky, "Dye-Doped Mesostructured Silica as a Distributed Feedback Laser Fabricated by Soft Lithography," Adv. Mater. **13**(16), 1231–1234 (2001).
12. D. Pisignano, L. Persano, E. Mele, P. Visconti, R. Cingolani, G. Gigli, G. Barbarella, and L. Favaretto, "Emission properties of printed organic semiconductor lasers," Opt. Lett. **30**(3), 260–262 (2005).
13. are P. Del Carro, A. Camposeo, R. Stabile, E. Mele, L. Persano, R. Cingolani, and D. Pisignano, "Near-infrared imprinted distributed feedback lasers," Appl. Phys. Lett. **89**(20), 201105 (2006).

#126247 - $15.00 USD Received 5 Apr 2010; revised 30 May 2010; accepted 30 May 2010; published 2 Jun 2010

14. D. Pisignano, L. Persano, P. Visconti, R. Cingolani, G. Gigli, G. Barbarella, and L. Favaretto, "Oligomer-based organic distributed feedback lasers by room-temperature nanoimprint lithography," Appl. Phys. Lett. **83**(13), 2545–2547 (2003).
15. M. Stroisch, T. Woggon, U. Lemmer, G. Bastian, G. Violakis, and S. Pissadakis, "Organic semiconductor distributed feedback laser fabricated by direct laser interference ablation," Opt. Express **15**(7), 3968–3973 (2007).
16. B. Jia, H. Kang, J. Li, and M. Gu, "Use of radially polarized beams in three-dimensional photonic crystal fabrication with the two-photon polymerization method," Opt. Lett. **34**(13), 1918–1920 (2009).
17. L. Persano, A. Camposeo, P. Del Carro, E. Mele, R. Cingolani, and D. Pisignano, "Very high-quality distributed Bragg reflectors for organic lasing applications by reactive electron-beam deposition," Opt. Express **14**(5), 1951–1956 (2006).
18. S. García-Revilla, M. Zayac, R. Balda, M. Al-Saleh, D. Levy, and J. Fernández, "1Low threshold random lasing in dye-doped silica nano powders," Opt. Express **17**(15), 13202–13215 (2009).
19. D. Donisi, R. Asquini, A. d'Alessandro, and G. Assanto, "Distributed feedback grating in liquid crystal waveguide: a novel approach," Opt. Express **17**(7), 5251–5256 (2009).
20. D. Wright, E. Brasselet, J. Zyss, G. Langer, and W. Kern, "Dye-doped organic distributed-feedback lasers with index and surface gratings: the role of pump polarization and molecular orientation," J. Opt. Soc. Am. B **21**(5), 944–950 (2004).
21. W. J. Wadsworth, I. T. McKinnie, A. D. Woolhouse, and T. G. Haskell, "Efficient distributed feedback solid state dye laser with a dynamic grating," Appl. Phys. B **69**(2), 163–165 (1999).
22. R. Harbers, P. Strasser, D. Caimi, R. F. Mahrt, N. Moll, B. J. Offrein, D. Erni, W. Bachtold, and U. Scherf, "Enhanced feedback in organic photonic-crystal lasers," Appl. Phys. Lett. **87**(15), 151121 (2005).
23. I. García-Moreno, A. Costela, M. Pintado-Sierra, V. Martín, and R. Sastre, "Enhanced laser action of Perylene-Red doped polymeric materials," Opt. Express **17**(15), 12777–12784 (2009).
24. C. Karnutsch, C. Pflumm, G. Heliotis, J. C. deMello, D. D. C. Bradley, J. Wang, T. Weimann, V. Haug, C. Gartner, and U. Lemmer, "Improved organic semiconductor lasers based on a mixed-order distributed feedback resonator design," Appl. Phys. Lett. **90**(13), 131104 (2007).
25. E. B. Namdas, M. Tong, P. Ledochowitsch, S. R. Mednick, J. D. Yuen, D. Moses, and A. J. Heeger, "Low Thresholds in Polymer Lasers on Conductive Substrates by Distributed Feedback Nanoimprinting: Progress Toward Electrically Pumped Plastic Lasers," Adv. Mater. **21**(7), 799–802 (2009).
26. M. Reufer, S. Riechel, J. M. Lupton, J. Feldmann, U. Lemmer, D. Schneider, T. Benstem, T. Dobbertin, W. Kowalsky, A. Gombert, K. Forberich, V. Wittwer, and U. Scherf, "Low-threshold polymeric distributed feedback lasers with metallic contacts," Appl. Phys. Lett. **84**(17), 3262–3264 (2004).
27. Z. Li, Z. Zhang, T. Emery, A. Scherer, and D. Psaltis, "Single mode optofluidic distributed feedback dye laser," Opt. Express **14**(2), 696–701 (2006).
28. N. Tsutsumi, and M. Yamamoto, "Threshold reduction of a tunable organic laser using effective energy transfer," J. Opt. Soc. Am. B **23**(5), 842–845 (2006).
29. V. Bulovic V, V. G. Kozlov, V. B. Khalfin, and S. R. Forrest, "Transform-limited, narrow-linewidth lasing action in organic semiconductor microcavities," Science **279**(5350), 553–555 (1998).
30. P. P. Yaney, D. A. V. Kliner, P. E. Schrader, and R. L. Farrow, "Distributed-feedback dye laser for picosecond ultraviolet and visible spectroscopy," Rev. Sci. Instrum. **71**(3), 1296–1305 (2000).
31. Y. Oki, S. Miyamoto, M. Maeda, and N. J. Vasa, "Multiwavelength distributed-feedback dye laser array and its application to spectroscopy," Opt. Lett. **27**(14), 1220–1222 (2002).
32. G. M. Gale, P. Ranson, and M. Denariez-Roberge, "Coherent spectroscopy with a distributed feedback dye laser," Appl. Phys. B **44**(4), 221–233 (1987).
33. S. C. Schulz, "Web Based Photonic Crystal Biosensors for Drug Discovery & Diagnostics," in *Vacuum & Coating*, P.68, May (2008).
34. F. C. Krebs, "Polymer solar cell modules prepared using roll-to-roll methods: Knife-over-edge coating, slot-die coating and screen printing," Sol. Energy Mater. Sol. Cells **93**(4), 465–475 (2009).
35. B. T. Cunningham, P. Li, S. Schulz, B. Lin, C. Baird, J. Gerstenmaier, C. Genick, F. Wang, E. Fine, and L. Laing, "Label-free assays on the BIND system," J. Biomol. Screen. **9**(6), 481–490 (2004).
36. B. T. Cunningham, and L. Laing, "Microplate-based, label-free detection of biomolecular interactions: applications in proteomics," Expert Rev. Proteomics **3**(3), 271–281 (2006).
37. I. D. Block, L. L. Chan, and B. T. Cunningham, "Large-area submicron replica molding of porous low-k dielectric films and application to photonic crystal biosensor fabrication," Microelectron. Eng. **84**(4), 603–608 (2007).
38. W. Zhang, N. Ganesh, P. C. Mathias, and B. T. Cunningham, "Enhanced fluorescence on a photonic crystal surface incorporating nanorod structures," Small **4**(12), 2199–2203 (2008).
39. N. Ganesh, W. Zhang, P. C. Mathias, E. Chow, J. A. N. T. Soares, V. Malyarchuk, A. D. Smith, and B. T. Cunningham, "Enhanced fluorescence emission from quantum dots on a photonic crystal surface," Nat. Nanotechnol. **2**(8), 515–520 (2007).
40. B. Park, and M. Y. Han, "Organic light-emitting devices fabricated using a premetered coating process," Opt. Express **17**(24), 21362–21369 (2009).
41. S. Y. Chou, P. R. Krauss, and P. J. Renstrom, "Nanoimprint lithography," J. Vac. Sci. Technol. B **14**(6), 4129–4133 (1996).

#126247 - $15.00 USD Received 5 Apr 2010; revised 30 May 2010; accepted 30 May 2010; published 2 Jun 2010

42. S. Y. Chou, P. R. Krauss, and P. J. Renstrom, "Imprint lithography with 25-nanometer resolution," Science **272**(5258), 85–87 (1996).
43. R. Hanumanthu, Scriven, and L. E., *Coating with patterned rolls and rods* (TAPPI, Norcross, GA, ETATS-UNIS, 1996).
44. C. Kallinger, M. Hilmer, A. Haugeneder, M. Perner, W. Spirkl, U. Lemmer, J. Feldmann, U. Scherf, K. Müllen, A. Gombert, and V. Wittwer, "A Flexible Conjugated Polymer Laser," Adv. Mater. **10**(12), 920–923 (1998).
45. G. Heliotis, R. Xia, G. A. Turnbull, P. Andrew, W. L. Barnes, I. D. W. Samuel, and D. D. C. Bradley, "Emission Characteristics and Performance Comparison of Polyfluorene Lasers with One- and Two-Dimensional Distributed Feedback," Adv. Funct. Mater. **14**(1), 91–97 (2004).

1. Introduction

Solid state organic lasers have attracted considerable attention since their first demonstration in 1967 by Soffer .el [1]. Because plastic-based lasers may be fabricated upon inexpensive substrates using fabrication approaches such as ink-jet printing to create patterned multilayer structures, they hold promise for applications that include optical communications, video display, and biosensors [2–4]. In addition to facilitating low manufacturing costs, fabrication upon flexible plastic substrates will enable lasers to be incorporated into curvilinear surfaces. Of the organic laser structures, the distributed feedback (DFB) laser has generated enthusiasm due to its wide wavelength range, compact structure, and compatibility with other thin film organic devices [5–10], with many recent efforts devoted to improving its performance and fabrication process while developing new applications [11–17]. These efforts have yielded new benchmarks for operation lifetime, lasing threshold, and emission stability [18–29].

Through the selection of the DFB grating period, grating height, material refractive indices, dye material, and gain layer thickness, single mode lasing output may be obtained with either horizontal or vertical emission for any desired wavelength from visible to near infrared [13,18,27]. While many DFB lasers are designed to emit a single (static) wavelength, it is also possible to create DFB lasers whose output wavelength may be dynamically tuned [6–8,10]. One such example was recently demonstrated by Lu, et. al. [3,4], in which the incorporation of biomolecules on the surface of an organic vertically emitting DFB laser, designed so that a portion of the lasing mode extended into a liquid medium, resulted in an increase of the lasing wavelength. In general, many applications for which optically pumped organic DFB lasers have been demonstrated, like sensing [3,4,18] and spectroscopy [10,30–32], would benefit from a fabrication approach that provides a path toward inexpensive manufacturing.

One of the most efficient manufacturing paradigms currently available involves "roll-to-roll" processing, in which a flexible substrate material is unwound from a compact cylindrical spool so that a series of fabrication processes can be performed in a continuous or stepwise manner, after which the substrate is wound upon a spool of "finished" material. Roll-based manufacturing is used for high volume, low cost, large surface area products, and can incorporate processes such as nanoreplica molding of quasi-three dimensional structures [33,34], dielectric thin film deposition, screen printing, and many others. After the roll-based processing is completed, individual parts may be cut from a roll using a die press or other automated cutting tool, and manipulated as individual pieces for assembly with other components. Due to the constraints of fabrication in a roll format, roll-based manufacturing is not compatible with the techniques (such as electron beam lithography) commonly used to obtain the submicron features of DFB lasers or techniques (such as spin-coating) that are used to obtain polymer films with precise submicron thickness. Roll-based fabrication upon plastic substrates is further constrained by the requirement not to exceed the softening temperature of the material, with a strong preference for processes that can be performed near room temperature.

In previous work, we have demonstrated a room temperature replica molding process for producing submicron grating features used for photonic crystal biosensors [35–37] and photonic crystal enhanced-fluorescence substrates for biochemical assays [38,39]. The process

#126247 - $15.00 USD Received 5 Apr 2010; revised 30 May 2010; accepted 30 May 2010; published 2 Jun 2010

for these devices involves roll-to-roll manufacturing of the grating structure, as well as roll-to-roll deposition of SiO_2 and TiO_2 sputtered dielectric thin films [33].

Recently, a novel process called "horizontal dipping" has been demonstrated as an effective method for producing thin polymer films used in organic light emitting diodes (OLED) [40]. In horizontal dipping, a reservoir of coating fluid is maintained between the substrate and a horizintal metal rod placed ~1 mm above the substrate by capillary action. By drawing the substrate underneath the rod, a thin film is deposited upon the substrate, in which the resulting film thickness is accurately controlled by the dilution of the polymer within the coating solvent and by the velocity of the substrate as it passes under the rod. Because horizontal dipping is easily controlled, performed at room temperature, and does not require substrate rotation, it is an ideal process for creating the dye-doped polymer waveguide region of a DFB laser.

In this paper, we report on the uniform, large-area fabrication of an organic DFB laser structure on a flexible plastic substrate, for which the DFB grating is produced by nanoreplica molding and the dye-doped waveguide region is produced by horizontal dipping. We focus mainly upon characterization of the horizontal dipping process, and characterize the relationship between the dipping speed and the thickness of the resulting polymer layer. Precise control and uniformity of the polymer waveguide layer is particularly important for the DFB laser, as a layer with thickness < 515 nm is required to obtain single mode output, and the laser output wavelength is dependent upon the waveguide thickness. Control of the waveguide thickness provides a means for obtaining any desired laser wavelength over a ~35 nm wavelength range, holding all other variables constant. Using a detection instrument that enables the spatial mapping of the laser wavelength over a ~10 cm^2 surface area, we demonstrate the uniformity of the replica molding/horizontal dipping process. Finally, we demonstrate that the horizontally-dipped waveguide layer may be easily patterned by photolithography to create distinct, isolated regions of DFB laser. While the application that motivates our research is the development of DFB laser biosensor surfaces for applications in life science research, pharmaceutical discovery, and diagnostic tests, the method presented here may be used to inexpensively fabricate any DFB laser structure for a broad range of applications.

2. Device design and fabrication process

A cross-sectional diagram of a representative vertically emitting organic DFB laser is shown in Fig. 1. The substrate is a flexible polyester (PET) film and the grating is formed in a layer of UV-curable polymer (UVCP) by a replica molding process. The corrugated UVCP layer functions as a distributed reflector and also as a cladding layer. Following the grating replication process, the grating surface is coated with a laser dye doped polymer layer using the horizontal dipping process. This layer is responsible for light amplification and also serves as a waveguide by providing light confinement. For a vertically emitting organic DFB laser or a second order distributed feedback laser, stimulated emission occurs at one band edge near the Bragg resonance, determined by the equation $m\lambda_{Bragg} = 2n_{eff}\Lambda$, where $m = 2$ is the order of diffraction, n_{eff} is the effective refractive index of the resonant mode, and Λ is the grating period. The effective refractive index depends on the thickness and refractive index of wave guidance layer, the refractive index of cladding layer and surrounding material. Therefore, single mode DFB lasers operating in a wavelength range as wide as 35.51 nm can be realized by precise control of the wave guidance layer thickness during the horizontal dipping process. The fabrication process is summarized schematically in Fig. 2.

#126247 - $15.00 USD Received 5 Apr 2010; revised 30 May 2010; accepted 30 May 2010; published 2 Jun 2010

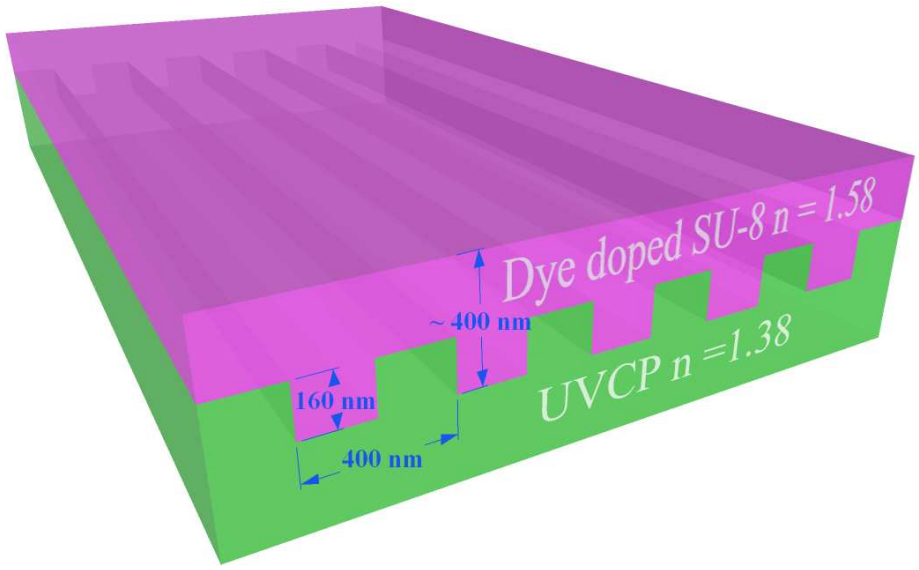

Fig. 1. Schematic diagram of the DFB laser structure.

2.1 Nano-replica molding process

To perform nano-replica molding, a master mold with negative image of the sub-wavelength grating was produced by nano-imprint lithography on an 8 inch-diameter Si wafer [41,42]. The patterned silicon wafer has a period of 400 nm, a duty cycle of 50%, and a depth of 160 nm. The silicon master mold was treated with Repel Silane (Amersham Biosciences) to facilitate mold separation. A small volume (~1ml) of liquid UV-curable polymer (WR354, SSCP CO., LTD.) was dispensed onto the silicon master wafer surface. After attaching a PET sheet, the liquid UVCP was squeezed between the master mold and the PET substrate with a ~5 lb. roller, enabling the UVCP to spread and fill the grating uniformly, while simultaneously eliminating trapped air pockets. The UV-curing process takes place under high intensity UV lamp (Xenon) exposure for ~90 seconds at room temperature. After curing, the silicon mold and the replica of the grating are separated by peeling the PET substrate away from the silicon mold such that the cured polymer grating preferentially and permanently adheres to the PET substrate. The cured polymer film has a refractive index of n = 1.38 at λ = 600 nm and a thickness ~5 μm. The patterned area is as large as 12 × 9 cm^2 with grating structure shown in Fig. 1.

#126247 - $15.00 USD Received 5 Apr 2010; revised 30 May 2010; accepted 30 May 2010; published 2 Jun 2010

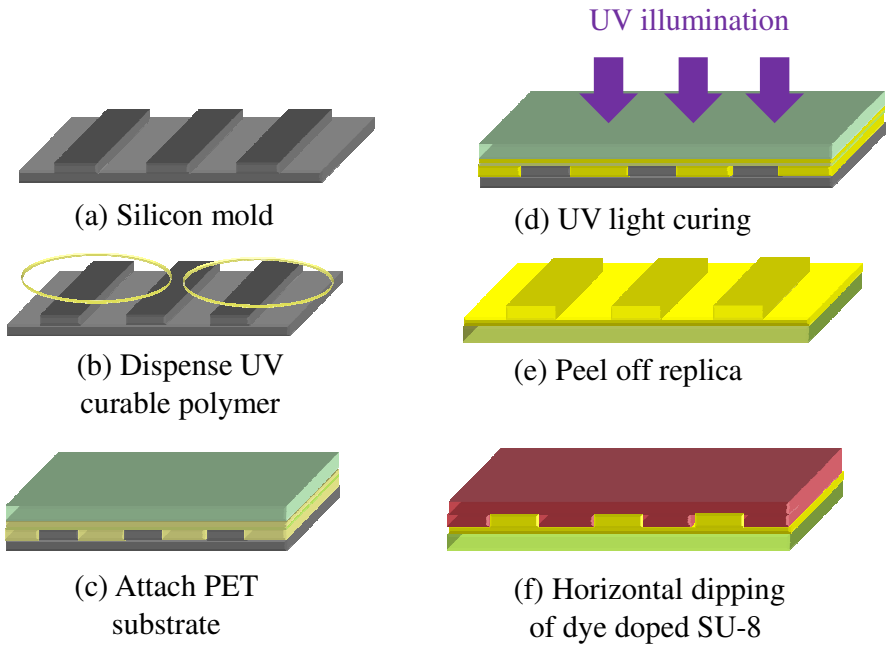

Fig. 2. Process flow diagram for the solid state organic DFB laser.

2.2 Horizontal dipping process

The horizontal dipping process is capable of coating organic film over a large thickness range on various substrates. The horizontal dipping method is categorized as a pre-metered coating technique, which means that the thickness of the coated film is determined by the process itself, unlike other coating techniques such as Knife Over Roll Coating [34], Air Knife Coating [34] or Metering Rod (Meyer Rod) Coating [43], for which the thickness of the coated film is determined by an external process. Given a specific substrate and coating material combination, there are two ways to control the thickness. The first method is to adjust the spacing between the cylindrical barrier and the substrate, while the second method is to control the translation speed of the carrier stage. In this experiment, the second method is adopted. The core component of the horizontal dipping setup is a stainless steel coating barrier (SUS Steel), which is a cylindrical rod with a radius of 0.25 inch. The coating barrier is mounted on a two dimensional (x and z) translation stage. The vertical stage is used to adjust the barrier height, h_0, with respect to the substrate surface. A motorized horizontal stage (SGSP 26-150, Optosigma) moves the coating barrier over the grating substrate with speed controlled by a programmable motor controller (SHOT-602, Optosigma).

Before the dipping process, the active polymer layer was prepared by mixing a 5 mg/ml solution of Rhodamine 590 dye (Exciton) in CH_2Cl_2 with SU-8 (5.0 wt %; Microchem) to a volume percentage of 10%. This mixture was sonicated for improved homogenization. The dye doped polymer solution was injected into the gap between the barrier and the substrate by a syringe. The solution spread in the gap by capillary action, and formed a downstream meniscus [34,40]. During the horizontal dipping process, the substrate was held horizontally on a vacuum chuck and the barrier translated smoothly at a preset speed, leaving a thin film of the dye doped solution on the grating substrate. After the dipping process, the coated device was soft baked on a 95 °C hotplate for 1 min to remove the solvent. After that, the SU-8 film was photopolymerized by exposing to UV radiation (λ = 365 nm lamp source) with exposure dose of 100 mJ cm^{-2}, and subsequently hard baked on a 95 °C hot plate for 2 min.

#126247 - $15.00 USD Received 5 Apr 2010; revised 30 May 2010; accepted 30 May 2010; published 2 Jun 2010

Using SU-8 with a viscosity of 7.5 cSt, the barrier height and the translation stage speed determine the coating thickness which, in turn, determines the stimulated emission wavelength of the DFB laser. The relationship between the film thickness and the translation speed was studied using an atomic force microscope (AFM) (Digital Instruments Dimension 3000 Atomic Force Microscope, Veeco) and an optical interferometry profiler (Veeco NT1000 optical profiler, Veeco). In addition, since the thickness of the gain layer is closely related to the stimulated emission wavelength, by measuring the laser emission spectrum as a function of the spatial location, we can also map out the spatial variation of the refractive index of the laser surface, so as to characterize the uniformity or surface morphology of the device.

2.3 Active layer pattern process

For some applications, it is useful to have a patterned device, in which selected regions of the surface are not capable of lasing action. Using SU-8 as the laser dye host allows us to easily pattern the light emission area in any shape using the conventional photolithography. As mentioned above, after the device was soft baked on a 95 °C hotplate for 1 min to remove the solvent, the device was photopolymerized by exposure to UV radiation (λ = 365 nm lamp source) through a photomask. To demonstrate this, we designed a photomask with the pattern of a Chinese character "中" which occupies a 1mm × 1mm area with a feature size of 125 μm. The exposed film was post-baked at 95 °C for 120 seconds and the unexposed area was removed by the developing process, resulting in a patterned area with a negative image of the pattern mask.

Previous work has shown that the nanoreplica molding process is capable of reproducing sub-wavelength grating structures over large surface areas [4], and implementation of a roll-to-roll process for high volume manufacturing [37]. We envision that the horizontal dipping process can be implemented as a process that can be performed in a roll-to-roll manner upon replica-molded grating structures either on a separate piece of manufacturing equipment, or integrated within a machine that can perform both processes.

3. Test instrumentation

Figure 3 shows a schematic diagram of the experimental setup used to characterize the performance of the fabricated DFB laser. Optical pumping was provided by a frequency-doubled, *Q*-switched Nd: YAG pulse laser (λ_p = 532 nm, yttrium aluminum garnet) with a pulse duration of 10ps at a maximum repetition rate of 10 Hz. The pumping beam passed through a spatial filter and a 10 × beam expander and a spatial filter to spatially clean the beam. Focused by a 10 × objective, the pumping beam formed a ~4 μm diameter spot on the DFB laser surface which was placed on the focal plane of the objective.

#126247 - $15.00 USD Received 5 Apr 2010; revised 30 May 2010; accepted 30 May 2010; published 2 Jun 2010

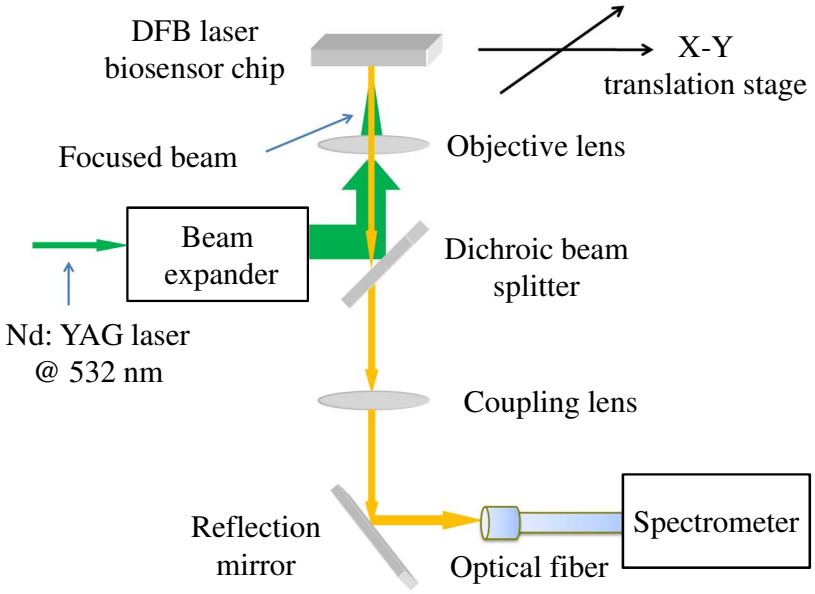

Fig. 3. Schematic diagram of the DFB laser detection instrumentation setup.

The lasing emission from the device was collected by the same objective and then passed through a dichroic mirror and a long pass emission filter that eliminated the strong pumping light. Because a 1D DFB resonator only provides confinement perpendicular to grating axis, the beam is highly divergent along the direction parallel to the grating axis [44,45]. To account for this effect, the stimulated emission was coupled into a step index multimode fiber (d = 600 μm, NA = 0.48) with a large numerical aperture (NA) using a convex lens. Finally, a spectrometer (iHR550, Horiba Jobin Yvon) with a 1800 lines/mm grating and a charge coupled device was used to analyze the emission spectrum. The measured laser emission was fitted with a Lorentzian distribution model to precisely determine the peak wavelength value (PWV).

4. Device characterization

4.1 Film thickness

For the horizontal dipping process, the coating polymer is categorized as a Newtonian liquid which is usually characterized by its viscosity, density, and surface tension. A downstream meniscus shape will form after the solution is fed into the gap between the stainless steel barrier and the grating surface. The relationship between the film thickness and the radius of the curvature of the downstream meniscus is given by Eq. (1):

$$t_w = 1.34(\frac{\mu U}{\sigma})^{2/3} \bullet R_d . \quad (1)$$

where R_d represents the radius of curvature of the downstream meniscus, μ and σ represent the viscosity and surface tension of the coating solution, respectively, and U is the carrying speed [40]. During the coating process, the gap between the stainless steel barrier and the grating surface was kept at 0.9 mm and the translation velocity of the barrier was adjusted from 0.01 cm/s to 0.8 cm/s. The resulting gain layer thickness ranged from 234.0 nm to more than 3.1 μm, as shown in Fig. 4. With the lowest translation speed of 0.01cm/s, a film thickness of ~234 nm was achieved. The film thickness is measured both by an atomic force microscope (AFM) (Digital Instruments Dimension 3000 Atomic Force Microscope, Veeco) and an

#126247 - $15.00 USD Received 5 Apr 2010; revised 30 May 2010; accepted 30 May 2010; published 2 Jun 2010

optical surface profiler (Veeco NT1000 optical profiler, Veeco). The measurement results are compared to the theoretical prediction, shown as the red curve in Fig. 4.

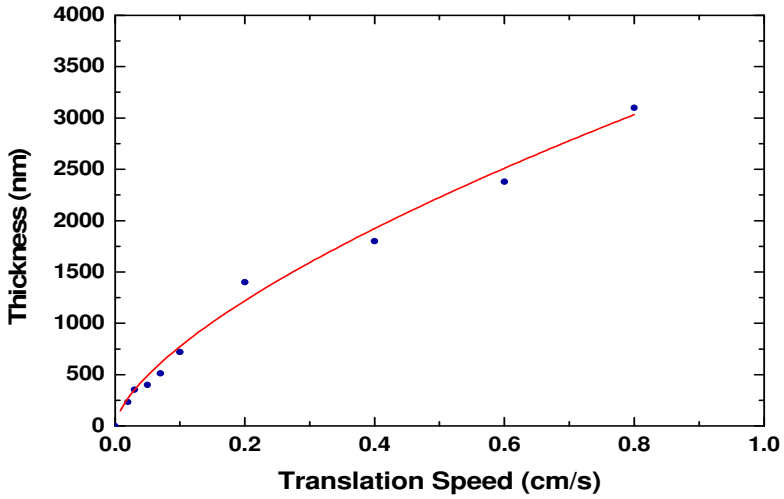

Fig. 4. Relationship between the translation speed of the carrier stage and the guidance layer thickness: the translation speed ranges from 0.01cm/s to 0.8cm/s and the corresponding film thickness ranges from 234nm to ~3.1μm.

4.2 DFB laser performance

Another advantage of this fabrication strategy is the wide tunability of the lasing emission wavelength. As mentioned in the device design section, the lasing wavelength could be tuned within the emission spectral region of the gain material by modifying the effective refractive index by controlling of the thickness of the wave guidance layer. The emission wavelengths of devices with different guidance layer thicknesses were measured, and are shown in Fig. 5. Since the guidance layer has a larger refractive index compared to the superstrate media and the substrate layer, an increase in the thickness of the guidance layer will introduce a red shift in the lasing emission wavelength. The relationship between the guidance layer thickness and the stimulated emission wavelength is depicted in the inset plot. Single mode emission was observed when the guidance layer thickness was within a range of 234-510 nm. When a much thicker guidance layer was employed, the laser began to emit multiple modes, as shown in the top left inset plot.

#126247 - $15.00 USD Received 5 Apr 2010; revised 30 May 2010; accepted 30 May 2010; published 2 Jun 2010

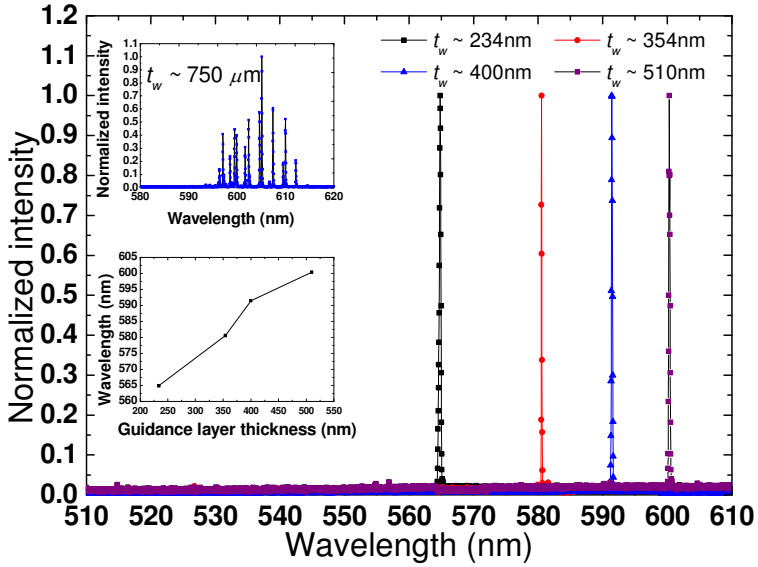

Fig. 5. Stimulated emission characteristics of devices with various guidance layer thicknesses (t_w). The fabricated lasers exhibit a linewidth of $\Delta\lambda = 0.15$ nm, threshold pump fluence ~0.169 mJ-cm^{-2} at $\lambda = 532$ nm. The top left inset picture shows multiple modes emission when the guidance layer thickness is ~750 μm. The bottom left inset plot shows the relationship between the laser emission wavelength and the guidance layer thickness.

4.3 Film thickness uniformity

Due to the relationship between the thickness of the guidance layer and the laser emission wavelength, the uniformity of the device can be investigated by measurement of the spatial distribution of stimulated emission wavelengths. The measurement results are shown in Fig. 6. The laser emission wavelength measurement was first performed in a line-by-line manner with 2mm spacing between adjacent sampling spots on a device having an area of 50mm × 20mm, as shown in the top of Fig. 6. The range of the PWV variation is $\Delta\lambda$~3.15nm, which indicates a variation range of ~36 nm of the guidance layer thickness according to rigorous coupled wave analysis (RCWA) simulations of the device structure (simulation results not shown). The standard deviation of PWV is 0.514nm, resulting in a coefficient of variation of CV = 0.087%. To characterize the uniformity with a finer spatial scale over a small surface area, a zoomed in measurement was performed in a single 2mm × 2mm square, with 125 μm spacing between adjacent sampling spots. As shown in the bottom of Fig. 6, the PWV range was $\Delta\lambda = 0.481$ nm, with a standard deviation of 0.129 nm and a coefficient of variation of CV = 0.022% The measured standard deviation of DFB output wavelength corresponds to only ~1.57 nm standard deviation of the guidance layer thickness over a 4 mm^2 area. These results were further verified by an AFM measurement.

#126247 - $15.00 USD Received 5 Apr 2010; revised 30 May 2010; accepted 30 May 2010; published 2 Jun 2010

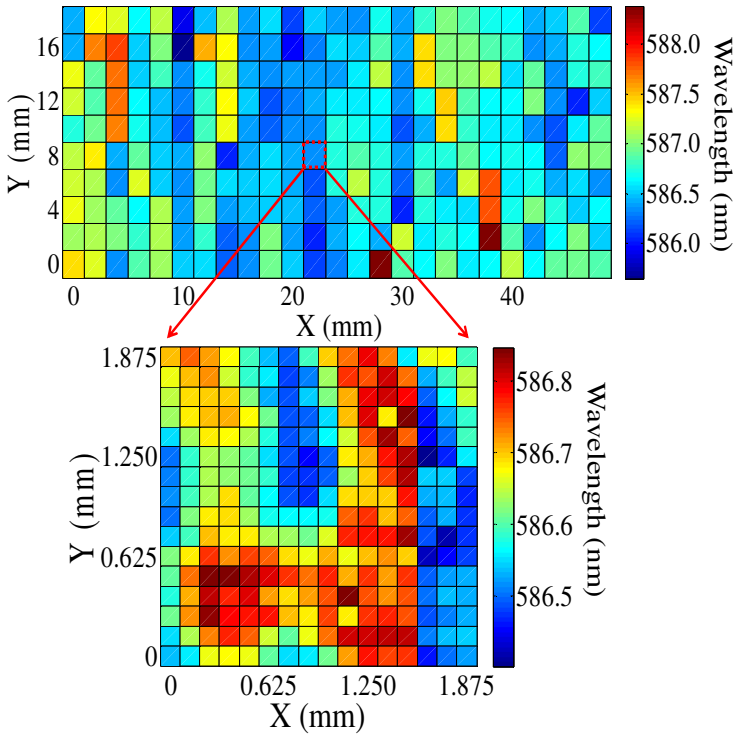

Fig. 6. Spatial distribution of the laser emission wavelength. The top picture illustrates a map of laser emission wavelength over a 5cm × 2 cm area. For such an area, the laser emission varies within a range of 3.15nm. The bottom picture shows a zoomed-in perspective of the lasing wavelength distribution within a single grid with a 2mm × 2 mm area, where the laser emission ranges from 586.41nm to 586.89nm.

4.4 Emission image of patterned DFB laser

In some applications, it is desirable for the laser light source to be patterned. For example, for our application for creating DFB laser biosensors, it is often desirable to create discrete regions of DFB laser surface that can be functionalized with different capture molecules for creating an array of small sensors that can be probed individually. Patterning by photolithography is an established fabrication process involving simple steps, including photoresist (PR) coating, PR baking, exposure, developing, material etching and PR stripping. Devices made by the method described in this work can be easily patterned using photolithography, while still in a roll-based format because the horizontal-dipped layer of the dye-doped SU-8 is photosensitive.

Figure 7 shows the spatial laser emission profile of a device with a patterned SU-8 layer, using the process described in Section 2.3, in which the mask was created by printing ink on a transparent plastic sheet with a laser printer. Since the laser-printed pattern has a feature resolution of 125 μm, the spatial resolution between the adjacent pumping spot was chosen to be 12.5 μm to satisfy the Nyquist sampling frequency. In Fig. 7, regions that do no lase are assigned a wavelength of 0 nm, and are displayed in black. The spatial distribution of the stimulated emission wavelength along the horizontal direction is also shown. The variation is within a $\Delta\lambda = 0.14$ nm range.

#126247 - $15.00 USD Received 5 Apr 2010; revised 30 May 2010; accepted 30 May 2010; published 2 Jun 2010

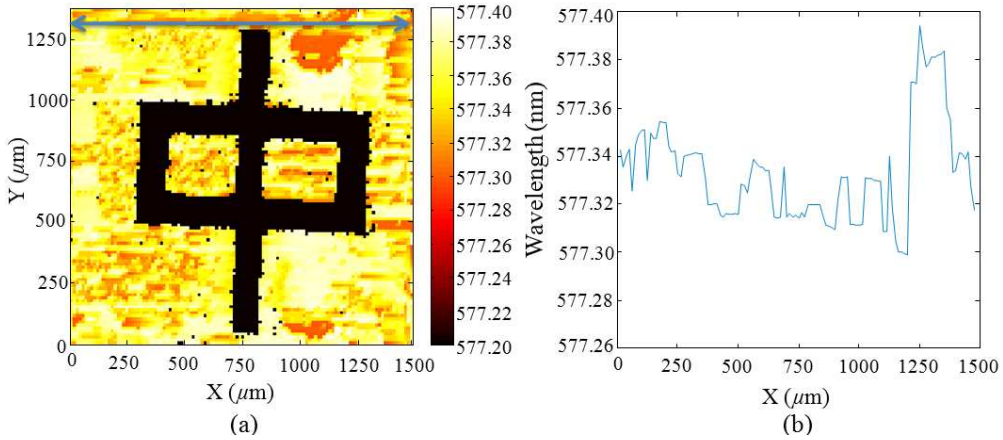

Fig. 7. Emission characteristics of a patterned DFB laser. (a) The stimulated emission image of a patterned DFB laser: The black part with a pattern "中" indicates the dumb region where the gain layer has been removed. So the laser does not lase there, while the laser works normally in the complementary region. The spatial resolution of the image is 12.5μm, and the feature size of the pattern is 125 μm. (b) The spatial distribution of the stimulated emission wavelength cross a horizontal line in (a): The variation of the lasing emission cross the horizontal line is within a 0.14 nm range, while the lasing wavelength difference between adjacent spots is less than 0.01 nm.

5. Conclusion

A fabrication method that combines nanoreplica molding and horizontal dipping processes has been developed for organic DFB lasers upon flexible plastic substrates. The spatially corrugated surface can be produced inexpensively and in virtually any periodicity upon a plastic substrate by the nano-replica molding method. The subsequent horizontal dipping process allows uniform coating of dye doped polymer active layer onto the grating surface at desired thickness ranging from 234.0 nm to 3.1 μm. Lasing from the polymer-based DFB structure, having a replicated Λ = 400 nm polymer grating and a Rhodamine 590 doped SU-8 active medium, has been demonstrated and characterized. The laser emission wavelength can be controlled in the λ = 564.82-600.33nm wavelength range. The tested DFB laser exhibits a linewidth of $\Delta\lambda$ = 0.15 nm, a threshold pump fluence ~0.169 mJ-cm^{-2} at λ = 532.00 nm, and emission wavelength variations as small as 3.15 nm over a 10 cm^2 area. From this example of a plastic DFB laser, it is clear that the developed fabrication method has the capability of producing organic DFB laser and organic DFB laser arrays for a wide range of wavelengths.

Acknowledgement

This project was made possible by a cooperative agreement that was awarded and administered by the U.S. Army Medical Research & Materiel Command (USAMRMC) and the Telemedicine & Advanced Technology Research Center (TATRC), under Contract #: W81XWH0810701. The authors also extend their gratitude to the support staff of Micro and Nanotechnology Laboratory at University of Illinois at Urbana-Champaign.

#126247 - $15.00 USD Received 5 Apr 2010; revised 30 May 2010; accepted 30 May 2010; published 2 Jun 2010